

## Simulations of combined ICRF and NBI heating for high fusion performance in JET

D. Gallart<sup>1</sup>, M.J. Mantsinen<sup>1,2</sup>, L. Garzotti<sup>3</sup>, R. Bilato<sup>4</sup>, C. Challis<sup>3</sup>, J. Garcia<sup>5</sup>,  
A. Gutierrez-Milla<sup>1</sup>, T. Johnson<sup>6</sup>, E. Lerche<sup>7</sup>, X. Sáez<sup>1</sup> D. Van Eester<sup>7</sup> and JET Contributors  
*EUROfusion Consortium, JET, Culham Science Centre, Abingdon, OX14 3DB, UK\**

<sup>1</sup> *Barcelona Supercomputing Center, Barcelona, Spain*

<sup>2</sup> *ICREA, Barcelona, Spain*

<sup>3</sup> *CCFE, Culham Science Centre, Abingdon, OX14 3DB, UK*

<sup>4</sup> *Max-Planck-Institut für Plasmaphysik, Garching, Germany*

<sup>5</sup> *CEA, IRFM, Saint-Paul-lez-Durance, France*

<sup>6</sup> *Euratom-VR Association, EES, KTH, Stockholm, Sweden*

<sup>7</sup> *Laboratory for Plasma Physics, LPP-ERM/KMS, Brussels, Belgium*

**Abstract** We report on simulations aimed at optimizing external heating using neutral beam injection (NBI) and radiofrequency waves in the ion cyclotron range of frequencies (ICRF) for high fusion yield in the JET tokamak. In this paper, D and DT plasmas are analyzed taking into account the NBI+RF synergy focusing on two different minority ICRF schemes, <sup>3</sup>He and H, respectively. Our results show that by increasing external heating power to the maximum power available, the fusion neutron rate can be enhanced in D plasma by a factor of 2-3 with respect to our reference record D discharge. Regarding the DT plasma we present the external heating performance under the variation of key plasma parameters. We also study the impact of the effects of ICRH to the fusion yield and show that the ICRH power results in an enhanced fusion yield in the whole parameter space studied.

**Introduction** NBI and ICRF heating are the main heating methods envisaged for bringing ITER plasmas to thermonuclear temperatures. In particular, we compare the performance of <sup>3</sup>He and H minority heating using the ICRF modelling code PION [1] coupled to the beam deposition code PENCIL [2] which both were coupled to the transport code JETTO [3]. PION + PENCIL modelling takes into account the synergy between ICRF waves and resonant NBI ions. For an optimal bulk ion heating we study the average fast ion energy  $E_{ave}$  generated by ICRF heating and compare it against the critical energy  $E_{crit}$ , the energy threshold at which fast ions deliver their energy equally among thermal ions and electrons. Below this energy fast ions slow down by ion-ion collisions and therefore enhancing bulk ion heating. In our

\*See the Appendix of F. Romanelli et al., Proceedings of the 25th IAEA Fusion Energy Conference 2014, Saint Petersburg, Russia

analysis we use the hydrogen minority resonance  $\omega = \omega_{cH} = 2\omega_{cD}$  and  $^3\text{He}$  minority resonance with  $\omega = \omega_{c^3\text{He}} = 2\omega_{cT}$ , where  $\omega$  is the frequency of the launched wave and the ion cyclotron frequency is defined as  $\omega_c = ZeB/(Am_p)$ . Here,  $Ze$  and  $Am_p$  are the ion charge and mass, respectively, and  $B$  is the confining magnetic field. PION results have been compared with other ICRF modelling codes such as TORIC+SSFPQL [4], SELFO [5] and TOMCAT [6] showing a good agreement.

**Fusion performance of D plasma at high input power** Figure 1 compares the experimental total fusion reaction rate of the reference discharge which has a total of 27 MW of external heating power with two simulated cases using coupled PION, PENCIL and JETTO modelling. In the simulated cases a higher total power of 40 MW is assumed while keeping the same plasma density as in the reference discharge. We set the toroidal field at  $B_T = 3.25$  T and the plasma current at  $I_p = 2.7$  MA. The input power consisted of 34 MW of D NBI and 6 MW of ICRF power, which is the maximum power foreseen to be available for the presently planned future JET experiments. As we can see in Fig 1, our simulations suggest that the peak fusion reaction rate can be increased by a factor of about 2-3 by increasing the total injected power by a factor of 1.48 to its maximum value. The plasma performance becomes low from  $t = 9$  s onwards as the high-power phase (7-9s) was limited by impurity accumulation and MHD.

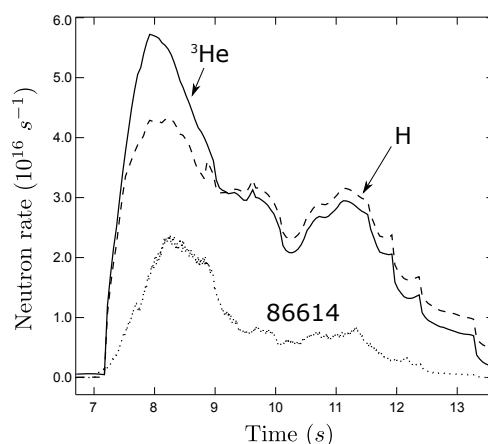


Figure 1: Neutron production rate (DD) for NBI+RF with a minority concentration of 4% in a deuterium plasma.

The two simulated scenarios in Fig. 1 have identical fuel mixtures except for the different minority ion species resonant with the launched waves. As we can see in Fig. 1, the  $\omega = \omega_{c^3\text{He}}$  scenario gives rise to a better fusion reactivity in the high performance phase as compared to the  $\omega = \omega_{cH} = 2\omega_{cD}$  scenario while the situation is opposite in the lower-performance phase.

In both scenarios, the ion temperature reaches its maximum at a minority concentration of about 4%, which are the cases considered in Fig. 1. However, the  $^3\text{He}$  scenario results in a higher ion temperature during all the NBI and ICRF phase with a maximum of 16 keV at the high performance phase and 12 keV on average at the low performance phase. Although the

H scenario gives rise to a lower temperature (12 keV at the high performance phase and 10 keV at the low performance phase), the synergy between the deuterium NBI and ICRF heating enhances the second deuterium harmonic damping and, thereby, the number of fast deuterons. This in its turn improves the fusion yield of the H minority scheme in the low performance phase as compared to that of the  $^3\text{He}$  scenario, although the extrapolation exercise is not as reliable as in the high performance phase due to non relevant plasma conditions.

**Combined NBI + ICRF heating in JET DT plasmas** We have performed an extensive series of simulations with coupled PENCIL and PION codes to study the dependence of the combined NBI + ICRF heating on key plasma parameters. We consider here a 50%-50% DT fuel ion mixture and we scan in plasma temperature and density of the reference discharge ( $n_e = 6.2 \times 10^{19} \text{ m}^{-3}$ ,  $T_e = 9 \text{ keV}$ ) assuming equal ion and electron temperatures. As in the previous case, the toroidal field is set to  $B_T = 3.25 \text{ T}$  and the plasma current to  $I_p = 2.7 \text{ MA}$ . The heating power consists of 34 MW of NBI power (17 MW of D and 17 MW of T) and 6 MW of ICRF power for the NBI+RF simulations. We also made the same set of simulations with NBI only, for comparison purposes.

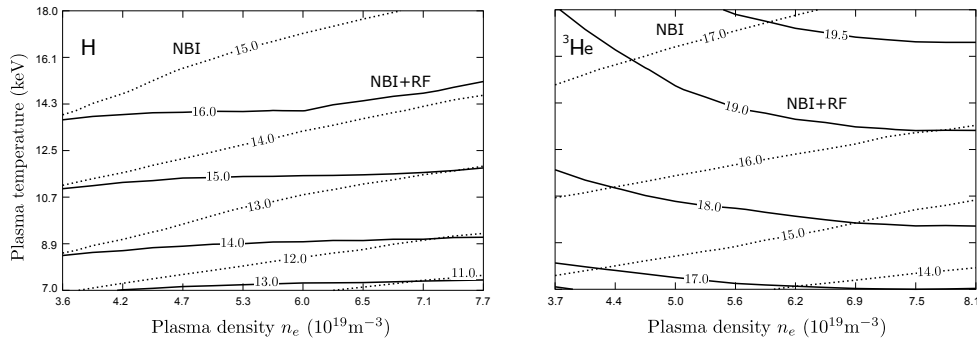


Figure 2: Collisional power for NBI and NBI+RF in MW for a minority concentration of 5%.

Figure 2 shows the collisional power to ions for both minority scenarios with NBI+RF power and NBI only. Notice that what we show is the collisional power to ions from the resonant species. Therefore, in the H scenario we show the D beams (17 MW and  $\sim 105 \text{ keV}$ ), which are resonant at the 2nd D harmonic resonance and in the  $^3\text{He}$  scenario we show the T beams (17 MW and  $\sim 95 \text{ keV}$ ), which are resonant at the 2nd T harmonic resonance. The density range under consideration allows the NBI to have a good penetration, hence, it reaches the plasma core. For all the range under consideration between 65-90% of the D NBI power and 82-100% of the T NBI power is transferred to ions. When adding ICRF the trend changes and the differences between the  $^3\text{He}$  and H minority scenarios grow. The NBI+RF collisional power to ions is mainly dependent on plasma temperature as the critical energy increases with  $T_e$ , hence, delivering more power to ions with increasing temperature. However, as compared to the NBI trend the NBI+RF collisional power to ions increases with the plasma density due to

two combined effects: the average energy of fast ions tends to decrease and the direct electron damping becomes relatively stronger for increasing plasma densities. Therefore, the proportion of average fast ion energy transferred to ions increases. Regarding the ICRF collisional power, it is roughly 20-30% higher in the  $^3\text{He}$  minority scenario. This is because of direct electron damping being  $\sim 20\%$  lower in the  $^3\text{He}$  minority scenario and the higher critical energy of  $^3\text{He}$ .

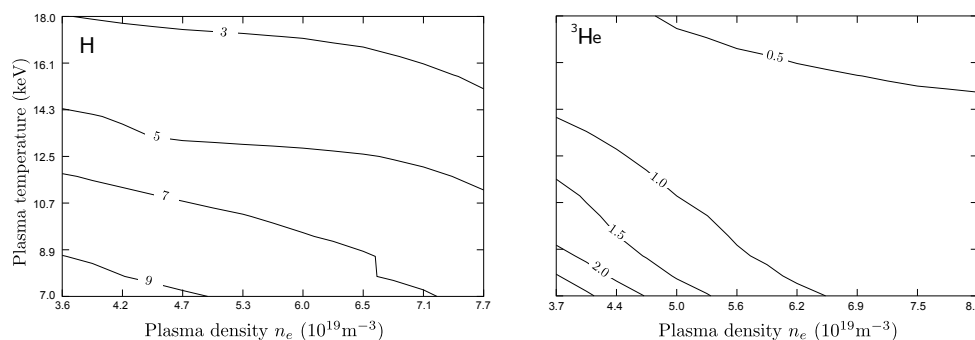


Figure 3: Enhancement in the D+T reaction rate from ICRF in % of the total  $\frac{R_{NT}(NBI+RF)-R_{NT}(NBI)}{R_{NT}(NBI+RF)}$ .

We have also modelled the effects of ICRF-accelerated tritons and deuterons on the D-T fusion reactivity (figure 3). The motivation for this study comes from the fact that, in principle, ICRF heating can accelerate deuterons and tritons beyond the optimal DT fusion reaction energy (120 keV), which could result in a lower fusion yield. Our modelling results summarized in figure 3 show, however, that this is not the case for the whole parameter range under consideration. Furthermore, we can see that the H scenario gives a higher ICRF enhancement of the D-T fusion yield than the  $^3\text{He}$  scenario. This is because the 2nd harmonic D absorption for the H minority scenario is 20-30% greater than the 2nd harmonic T absorption for the  $^3\text{He}$  minority scenario. Nevertheless both scenarios show similar trends: the ICRF enhancement is largest at low plasma density and temperature (9% and 2% for the H and  $^3\text{He}$  scenario, respectively) and becomes relatively smaller at high plasma density and temperature (3 and 0.5%, respectively) as the thermal fusion reactivity increases.

**Acknowledgments** This work has been carried out within the framework of the EUROfusion Consortium and has received funding from the Euratom research and training programme 2014-2018 under grant agreement No 633053. The views and opinions expressed herein do not necessarily reflect those of the European Commission. Dani Gallart would like to express his gratitude to “La Caixa” for support of his PhD studies.

## References

- [1] L.-G. Eriksson, T. Hellsten and U. Willén, Nuclear Fusion **33**, 1037 (1993).
- [2] P.M. Stubberfield and M.L. Watkins, Multiple Pencil Beam, JET-DPA(06)/87, 1987.
- [3] M. Romanelli, *et al.*, Plasma and Fusion Research 9, 3403023, 2014.
- [4] R. Bilato *et al.*, Nuclear Fusion **51** (2011) 10.
- [5] T. Hellsten *et al.*, Nucl Fusion **44** (2004) 892.
- [6] Van Eester and Koch, Plasma Phys. Control. Fusion **40** 1949 (1998).